EEG Recording During fMRI Experiments: Image Quality

K. Krakow,[1] P.J. Allen,[2] M.R. Symms,[1] L. Lemieux,[1]* O. Josephs,[3] and D.R. Fish[1,2]

[1]*Epilepsy Research Group, Department of Clinical Neurology, Institute of Neurology, University College London, Queen Square, London, and National Society for Epilepsy, Chalfont St. Peter, Bucks, UK*
[2]*Department of Clinical Neurophysiology, The National Hospital for Neurology and Neurosurgery, Queen Square, London, UK*
[3]*Wellcome Department of Cognitive Neurology, Functional Imaging Laboratory, Institute of Neurology, University College London, Queen Square, London, UK*

Abstract: Electroencephalographic (EEG) monitoring during functional magnetic resonance imaging (fMRI) experiments is increasingly applied for studying physiological and pathological brain function. However, the quality of the fMRI data can be significantly compromised by the EEG recording due to the magnetic susceptibility of the EEG electrode assemblies and electromagnetic noise emitted by the EEG recording equipment. We therefore investigated the effect of individual components of the EEG recording equipment on the quality of echo planar images. The artifact associated with each component was measured and compared to the minimum scalp-cortex distance measured in normal controls. The image noise originating from the EEG recording equipment was identified as coherent noise and could be eliminated by appropriate shielding of the EEG equipment. It was concluded that concurrent EEG and fMRI could be performed without compromising the image quality significantly if suitable equipment is used. The methods described and the results of this study should be useful to other researchers as a framework for testing of their own equipment and for the selection of appropriate equipment for EEG recording inside a MR scanner. *Hum. Brain Mapping 10:10–15, 2000.*

Key words: fMRI; EEG; electrophysiological recording; image quality; echo planar imaging; artifact; materials; epilepsy; multimodal imaging

INTRODUCTION

The recording of electroencephalograms (EEG) inside the MR scanner has gained increasing interest. It is used to correlate functional magnetic resonance imaging (fMRI) acquisitions with spontaneous EEG events (e.g., epileptiform discharges in patients with epilepsy and physiological EEG events such as oscillatory rhythms) or evoked potentials and thus help to identify the generators of these events [Huang-Hellinger et al., 1995; Krakow et al., 1999; Seeck et al., 1998; Warach et al., 1996]. A further application is monitoring the state of arousal or sleep during fMRI experiments [Portas et al., 1999].

EEG recording inside the magnetic fields of a MR scanner is associated with significant technical problems. Safety issues [Lemieux et al., 1997] and EEG

Contract grant sponsor: Medical Research Council, UK.

Correspondence to: Dr. Louis Lemieux, MRI Unit, National Society for Epilepsy, Chalfont St. Peter, Buckinghamshire SL9 0RJ, UK. E-mail: l.lemieux@ion.ucl.ac.uk

Received for publication 11 May 1999; accepted 3 February 2000

quality aspects [Allen et al., 1998] have already been addressed, providing the basis for high quality and safe EEG recordings inside the MR scanner. However, the effect of the EEG recording equipment on the MRI quality, particularly echo planar imaging (EPI), has not yet been addressed in detail. We therefore investigated two effects of the EEG recording, which can compromise MRI data: (1) Local signal drop out and geometric distortion due to magnetic susceptibility differences and the presence of eddy currents in EEG electrode assemblies [Joseph et al., 1996]; (2) Degradation of the image signal-to-noise ratio because of electromagnetic noise emitted by the EEG recording equipment.

The main purpose of this study was to evaluate these effects on a representative sample of EEG recording components to identify the most appropriate components for our setting, and to provide a general framework that can be useful to other researchers interested in evaluating their own equipment for EEG recording inside a MR scanner.

MATERIALS AND METHODS

All imaging was performed on a 1.5 T Horizon EchoSpeed MRI scanner (General Electric, Milwaukee, USA) unless stated otherwise.

Measurement of the scalp-cortex distance

T1-weighted inversion-recovery prepared volume acquisitions as used in our standard scanning protocol (Fast IRSPGR: TI/TR/TE/flip = 450/15/4.2/20; 124 1.5-mm thick coronal slices; 256 × 192 matrix, 24 × 18 cm FOV) of ten healthy volunteers were acquired (four males, six females, median age 36.0, range 17–50 years). The distance between the surface of the scalp and the cortex was measured at locations corresponding to the position of the FP1, F3, F7, C3, T3, P3, T5 electrodes of the 10/20 system, using our image display and analysis software, *MRreg* [Moran et al., 1999].

The following three experiments were carried out using a gradient-echo EPI sequence similar to the one we have used in clinical fMRI experiments [Krakow et al., 1999]: TR/TE = 3000/40, bandwidth 100 kHz, 24 cm FOV, flip angle 90, acquisition matrix 96 × 96, reconstruction matrix 128 × 128. Fat saturation was explicitly selected to prevent the scanner from using the spectral spatial pulse. Twenty contiguous 5-mm slices were acquired in an interleaved fashion.

Quantification of the local signal drop out and geometric distortions on a phantom

The following components of EEG electrode assemblies were assessed: electrodes, conductive electrode gel and paste, electrode adhesive, current-limiting resistors, insulating sleeve enclosing the resistor, and wire. Details of the origin and composition of the components are given in Table I. Each component was attached individually on the surface of a 10-cm glass sphere filled with distilled water. Electrodes, resistors, and wires were tested both with their long axis parallel (placed on top of the phantom, axial sections) and perpendicular (frontal side of phantom, coronal sections) to the B_0 magnetic field. Adhesive and gel were only tested on top of the phantom for practical reasons. All objects were scanned twice in each position on different occasions. Measurements were also made with the whole electrode assembly attached to the phantom. The maximum perpendicular depth of artifacts was measured in the images using *MRreg*.

Quantification of artifacts in vivo for the components with acceptable artifacts as measured in the phantom experiments

Electrode assemblies (consisting of an electrode, resistor, resistor insulation, wire, and 0.1 ml of electrode adhesive and gel) made of the components which gave acceptable results in the first experiment where placed on the right side of the scalp of a volunteer at the 10/20 electrode positions used in our clinical studies (FP2, F8, T4, T6, O2) [Krakow et al., 1999]. These were compared to electrode assemblies made up of nonoptimized components which have been used previously for intra-MR EEG (Ag/AgCl electrode, carbon current-limiting resistor, silicone-insulated copper lead) [Krakow et al., 1998], which were placed at the equivalent positions on the left side of the head. Images were obtained using a high resolution EPI (sequence parameters as above, except matrix size: 256 × 256). The depth of the artifact was measured using *MRreg*.

Quantification of the image noise caused by the electromagnetic fields generated by the EEG recording equipment

The EEG recording system consisted of electrode assemblies, placed in the headcoil beneath the phantom and connected to a non-ferrous headbox (developed in-house) located at the entrance to the bore of the magnet (headcoil-headbox distance = 125 cm). The headbox was connected to an unscreened battery-

TABLE I. Artifact measurements in phantom

Component description	Material/design	Artifact size (mm)
Electrodes		
Ag/AgCl: SLE UK; 131/9/TP	cast pure Ag coated in AgCl; d: 9 mm	8/8
Au: Grass USA; E5GH	cast pure Ag with heavy Au coating; d: 10 mm	6/4
Plastic Ag/AgCl: Meditec Italy; 1183 AGCL	plastic coated in Ag/AgCl; d: 10 mm	4/4
Carbon: Telefactor USA; carbon electrodes	carbon electrodes with carbon wire; d: 10 mm	2/4
Resistors		
Carbon composition: Vitrohm Germany; series BT, 104-0	carbon black, phenol resin, bakelite; length: 9.9 mm, d: 3.5 mm	19/19
Planar thick film cermet, BI Technology, BPCE	ruthenium oxide on aliminia substrate; 25.4/10.2/2.5 mm	6/4
Cermet film: Meggitt CGS; HB01	cermet film on ceramic substrate with epoxy coating; 26.5/10.5/3.0 mm	2/2
Resistor insulation		
Epoxy	rapid setting two part epoxy; 0.1 ml	8/8
Epoxy putty	0.1 ml	13/13
Heatshrink, black	irradiated polyolefin tubing; d: 9.5 mm	2/2
Leads		
Copper wire 1	annealed copper stranded wire, silicone rubber insulation; 128/0.05	2/2
Copper wire 2	silver plated copper stranded wire, PTFE insulation; 7/0.12	2/2
Carbon wire		0/0
Electrode adhesives/gels		
Collodion Adhesive: SLE UK	0.1 ml	4/4
Electrode gel: Dracard ECG Gel, Crown Graphic UK	0.1 ml	9/9
Elefix electrode paste: Nihon Kohden	combined adhesive/gel 0.1 ml	8/6

Ag: silver, AgCl: silverchloride, Au: gold. Dimensions of components: length/width/height, d: diameter. The two values in the third column represent the results of the two measurements.

powered Neurolink Patient Module (Physiometrix, MA, USA), placed at the side of the MR scanner (distance to the bore of the magnet: 130 cm). This digitizes and transmits the EEG signal out of the scanner room via a fiber optic cable to the Neurolink Monitor Module which reconstructs the analog EEG signals [Allen et al., 1998]. Phantom images were acquired with the (a) unshielded Patient Module switched off, (b) the unshielded Patient Module switched on, and (c) the Patient Module switched on, shielded with a double-walled aluminium/plastic box and a RF-filter in-line with all wires connecting to this box.

To measure the noise emitted by the EEG equipment, the EPI sequence was used with flip angle = 0 to measure that no RF energy was emitted from the scanner, giving an image containing only noise. This allowed us to detect any structured noise that may result from the EEG equipment. As the radiation that may be emitted by the EEG equipment has an unknown bandwidth, this experiment was repeated in a 2 T scanner (MAGNETOM Vision, Siemens, Erlangen, Germany) using the same EEG recording equipment. The mean and peak intensities over the whole image were measured using Dispimage [Plummer, 1992].

RESULTS

Scalp-cortex distance

The mean distance between surface of the scalp and the cortex measured was 13.8 mm (SD = 3.5). The smallest individual scalp-cortex distance, measured over the position T5, was 7.5 mm.

Local signal drop out and geometric distortions on a phantom

The pattern of signal drop out and geometric distortion of the phantom image caused by the tested objects was dependent on their spatial orientation with respect

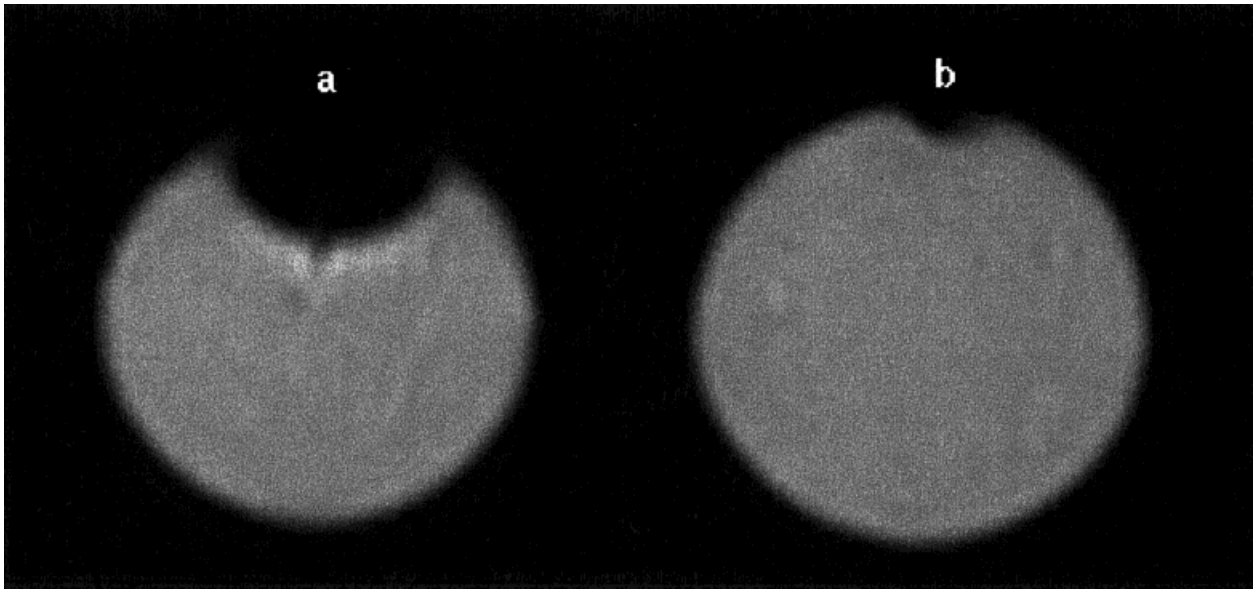

Figure 1.

Examples of image artifacts caused by current-limiting resistors as used in electrode assemblies. The images show the signal drop out/geometric distortion caused by the carbon composition resistor (**a**), and by the cermet film resistor (**b**), placed on the top of the phantom (diameter 10 cm).

to the B_0 magnetic field. The figures given in the last column of Table I represent the maximal depth of the artifact caused by the components placed on top of the phantom and orientated parallel to the B_0 vector. Artifacts were slightly more pronounced (< 20% increase in depth) if the long axis of objects was at right angle to the main magnetic field. The image artifacts caused by carbon, plastic covered silver and gold electrodes were within acceptable range (smaller than the minimum scalp-cortex distance in normal controls). Ag/AgCl electrodes caused slightly larger artifacts (Table I).

The different types of resistor showed significant differences. Carbon resistors caused an artifact intruding almost 20 mm into the phantom. Two planar cermet resistors gave satisfactory results with artifacts less than 2 and 6 mm in depth, respectively (Fig. 1). All leads tested resulted in negligible artifacts (< 2 mm).

Although the tested collodion adhesive caused an artifact intruding less than 4 mm, even minute amounts of conductive electrode gel (0.1 ml) led to artifacts of almost 10 mm depth. For the materials commonly used to insulate the resistor and improve the mechanical strength of the electrode assembly, epoxy putty gave the largest artifact (> 10 mm depth). When single components were combined to form electrode assemblies, the extent of the artifact was comparable to that of the worst single component.

Artifacts in vivo for the components with the smallest artifact as measured in the phantom experiments

EP-images of a volunteer with the optimized electrode assemblies demonstrated artifacts in superficial scalp tissue only (maximal depth < 5 mm), whereas nonoptimised electrode assemblies showed artifacts intruding the cortex (maximal depth > 15 mm) (Fig. 2).

Image noise caused by the electromagnetic fields generated by the EEG recording equipment

With the EEG equipment switched off (baseline) no image artifact was visible. The mean background noise was 10.5 (SD = 7.3) with a maximum intensity of 55.0. When the EEG digitizer (Patient Module) was switched on without shielding, the images were compromised by coherent noise. Approximately 0.3% of pixels had an intensity above background noise, forming a checkered design. The mean signal was 15.2 (SD = 18.6), the maximum signal, measured in the brightest pixels, was 538.0. When the shielding was applied to the Patient Module, no noise was detectable and the signal was in the range of the baseline-measurements (mean 10.1 (SD = 7.2), maximum 60.0). Similar results were obtained at 2 T.

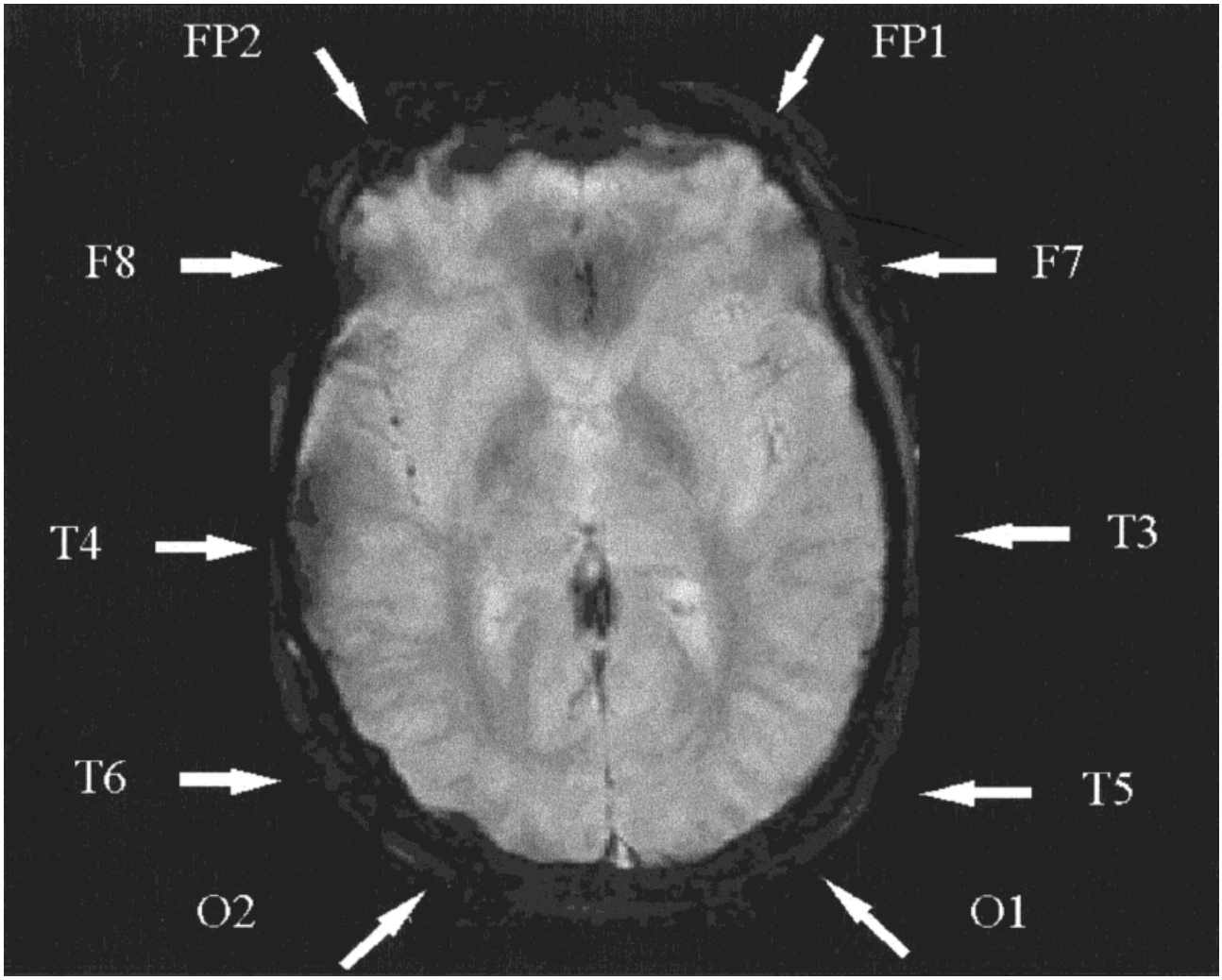

Figure 2.

Axial high resolution EPI of a subject with two chains of MR-compatible EEG electrode assemblies applied on the same electrode positions as in clinical studies. On the right side of the head (electrode positions FP2, F8, T4, T6, O2), nonoptimized electrode assemblies (Ag/AgCl electrodes, carbon composition resistor) caused artifacts intruding into the cortex. Optimized electrode assemblies (Au electrodes, cermet film resistor) used on equivalent positions on the left side of the head did not compromise the cortical signal. Both electrode assemblies contained identical copper leads, heatshrink resistor insulation, and 0.1 ml of Dracard electrode gel.

DISCUSSION

All components of the electrode assemblies tested caused some signal drop out and geometric distortions. In some cases, these exceed the minimum scalp-cortex distance as measured in a population of normal subjects (7.5 mm), thus potentially degrading the fMRI results. We found large differences in the artifact depth between components indicating the need to test carefully all objects intended to be used in electrode assemblies.

Most types of electrode gave image artifacts less than 7.5 mm. Although the smallest artifact was found in carbon and plastic electrodes, there are practical difficulties associated with constructing electrode assemblies from these as they cannot be soldered (for example, to connect the electrode to the current-limiting resistor). We found that the gold electrode gave the optimum combination of small artifact and ease of use.

There were large differences in artifacts for different resistor types. Many resistors use iron end caps (ferromagnetic) or nickel (paramagnetic) to attach the wire to the resistive material. These resistors were not included in this study, as they would necessarily lead to unacceptable artifacts. It is worth noting that the carbon compo-

sition resistor tested, in spite of being composed mainly of carbon, gave unacceptably large artifacts.

Some means of insulation of the resistors and wires from the patient is required and we have shown that a specific heat shrink sleeving could be used without causing a significant artifact. However, injecting epoxy into the sleeving around the resistor leads (to improve the mechanical strength of the lead-to-resistor joints) gave large artifacts and should be avoided. On the other hand, the wires tested caused only small artifacts and this suggests that carbon leads do not offer a significant advantage over metallic wire, but have two disadvantages: poor mechanical strength and difficulty in connecting to other parts of the electrode assembly.

Conductive gel gave large image artifacts, and as it can be expected that the depth of the signal drop-out and geometric distortion increases with larger amounts of gel, only the minimum amount necessary to give acceptable electrode impedance should be used.

A phantom was used for these measurements to facilitate quantification of the image artifacts and a comparison between the various components of EEG electrode assemblies. However, we found that the magnitude of the image artifacts in vivo were of similar depth to those on the phantom. Optimized electrode assemblies led to artifacts clearly smaller than the minimum scalp-cortex distance. We therefore conclude that EEG can be recorded inside a MR scanner without compromising the cortex signal by local artifacts.

With regard to electromagnetic noise emitted by the EEG equipment, we found significant coherent noise in the images if no shielding was used. This is presumably because of broadband signals generated by fast switching signals in the EEG digitizing circuit in the frequency range detected by the receiver chain of the MRI scanner. This noise is likely to be dependent on the type of the EEG equipment, its location in respect to the headcoil, and the scanner Larmor frequency (i.e., field strength). To illustrate this, we measured the noise level at two different field strengths (1.5 T and 2 T) and found it to be comparable in this case. By using an appropriate shielding device (aluminum box and RF filter) the noise could be removed completely for both field strengths.

Although we have tested a representative range of MR compatible components, it has to be emphasized that subtle changes in their manufacture process (e.g., modification of composition) or differences between manufacturers can cause significant changes of the MR-related material properties. The same applies for the EEG-recording module as a source of electromagnetic noise. The results of this study should therefore be seen only as a primary guideline for the selection of EEG recording equipment and a framework for an individual testing of components. We hope that the methods proposed in this work can be useful to other researchers who would like to assess the EEG/MRI compatibility of the their own equipment.

CONCLUSIONS

Concurrent EEG and fMRI can be carried out without compromising the image quality significantly if appropriate materials are chosen and precautions to shield electromagnetic noise are taken.

REFERENCES

Allen PJ, Polizzi G, Krakow K, Fish DR, Lemieux L. 1998. Identification of EEG events in the MR scanner: The problem of pulse artifact and a method for its subtraction. Neuroimage 8:229–239.

Huang-Hellinger FR, Breiter HC, McCormack G, Cohen MS, Kwong KK, Sutton JP, Savoy RL, Weisskoff RM, Davis TLD, Baker JR, Belliveau JW, Rosen BR. 1995. Simultaneous functional magnetic resonance imaging and electrophysiological recording. Hum Brain Mapp 3:13–23.

Joseph PM, Atlas SW. 1996. Artifacts. In: Atlas SW, editor. Magnetic resonance imaging of the brain and spine (2nd Ed.). Philadelphia: Lippincott-Raven, p 149–177.

Krakow K, Symms MR, Woermann FG, Allen PJ, Polizzi G, Fish DR. 1998. Reproducible localisation of interictal activation in epilepsy patients using spike-triggered fMRI. Neuroimage 7:S288.

Krakow K, Woermann FG, Symms MR, Allen PJ, Lemieux L, Barker JS, Duncan JS, Fish DR. 1999. EEG-triggered functional MR of interictal epileptiform activity in patients with partial seizures. Brain 122:1679–1688.

Lemieux L, Allen PJ, Franconi F, Symms MR, Fish DR. 1997. Recording of EEG during fMRI experiments: Patient safety. Magn Reson Med 35:943–952.

Moran NF, Lemieux L, Maudgill DD, Kitchen ND, Fish DR, Shorvon SD. 1999. Analysis of temporal lobe resections in MR images. Epilepsia 40:1077–1084.

Plummer DL. 1992. Dispimage: A display and analyse tool for medical images. Rev di Neuroradiol (Italy) 5:489–495.

Portas CM, Krakow K, Allen PJ, Josephs O, Frith C. 1999. Sensory processing across the sleep-wake cycle: A functional MRI study in humans. Society for Neuroscience, Abstracts 29th Annual Meeting 25(2):2065.

Seeck M, Lazeyras F, Michel CM, Blanke O, Gericke CA, Ives J, Delavelle J, Golay X, Haenggeli CA, de Tribolet N, Landis T. 1998. Non-invasive epileptic focus localization using EEG-triggered functional MRI and electromagnetic tomography. EEG Clin Neurophysiol 106:508–512.

Warach S, Ives JR, Schlaug G, Patel MR, Darby DG, Thangaraj V, Edelmann RR, Schomer DL. 1996. EEG-triggered echo-planar functional MRI in epilepsy. Neurology 47:89–93.